VASCULAR BIOLOGY

Oligo-guanosine nucleotide induces neuropilin-1 internalization in endothelial cells and inhibits angiogenesis

Masashi Narazaki,[1,2] Marta Segarra,[1] Xu Hou,[3] Toshio Tanaka,[2] Xuri Li,[3] and Giovanna Tosato[1]

[1]Laboratory of Cellular Oncology, Center for Cancer Research, National Cancer Institute, National Institutes of Health, Bethesda, MD; [2]Department of Respiratory Medicine, Allergy and Rheumatic Diseases, Osaka University Graduate School of Medicine, Osaka, Japan; and [3]National Eye Institute, Porter Neuroscience Research Center, National Institutes of Health, Bethesda, MD

Ligand interaction with cognate cell-surface receptor often promotes receptor internalization, protecting cells from prolonged or excessive signaling from extracellular ligands. Compounds that induce internalization of surface receptors prevent ligand binding to cognate cell-surface receptors serving as inhibitors. Here, we show that synthetic polyriboguanosine (poly G) and oligodeoxyriboguanosine (oligo G) reduce endothelial levels of surface neuropilin-1 (NRP1), a receptor shared by semaphorin 3A and vascular endothelial growth factor (VEGF), which plays critical roles in angiogenesis. Oligo G also reduces levels of cell-surface scavenger receptor expressed by endothelial cells I (SREC-I), but not levels of NRP2, gp130, CD31, VEGFR-1, or VEGFR-2. Poly or oligo A, T, and C do not promote NRP1 or SREC-I internalization. We find that oligo G binds to NRP1 with high affinity (Kd: 1.3 ± 0.16nM), bridges the extracellular domain of NRP1 to that of SREC-I, and induces coordinate internalization of NRP1 and SREC-I. In vitro, oligo G blocks the binding and function of $VEGF_{165}$ in endothelial cells. In vivo, intravitreal administration of oligo G reduces choroidal neovascularization in mice. These results demonstrate that synthetic oligo G is an inhibitor of pathologic angiogenenesis that reduces cell-surface levels and function of NRP1 acting as an internalization inducer. (*Blood*. 2010;116(16):3099-3107)

Introduction

Cell-surface receptors regulate cell responses by transmitting signals from soluble mediators, cell-surface molecules of adjacent cells, or extracellular matrix.[1-3] Expression levels of cell-surface receptors are controlled by transcriptional, epigenetic, and posttranscriptional regulation, which is dependent upon a variety of factors, including cell type, stage of cell differentiation, and surrounding environment clues. Receptor levels are also controlled by internalization, degradation, and recycling of cell-surface receptors.[4,5] Ligand binding to cognate receptors usually induces receptor internalization and signaling, which coordinately reduces cell-surface receptor levels and prevents further ligand binding. This mechanism can protect cells from prolonged or excessive signaling from cell-surface ligands.[4,6]

Neuropilin-1 (NRP1) is an endothelial cell receptor shared by class 3 semaphorins and vascular endothelial growth factor A (VEGF-A) isoform $VEGF_{165}$.[7-9] Genetic studies have provided strong evidence that NRP1 is required for normal vascular development, as NRP1-deficient mice display severe defects of vascular branching and remodeling.[10] The administration of NRP1 neutralizing antibodies to adult mice inhibited tumor angiogenesis and tumor growth.[11]

Structurally, NRP1 has an extracellular, a single transmembrane, and a short cytoplasmic domain. The extracellular domain of NRP1 includes 3 subdomains: the a1/a2 (CUB) domain at the N terminus with homology to complement components, followed by the b1/b2 (coagulation factor V/VIII) domain and the c (C-terminal MAM) domain.[12] Semaphorin 3A (Sema3A) binds to the a1/a2/b1 domains, whereas $VEGF_{165}$ binds to the b1/b2 domain.[13,14] In previous studies, we have shown that ligand (Sema3A or $VEGF_{165}$) interaction with NRP1 selects for the specific signal transducer chain, plexins for semaphorins or VEGF receptors for $VEGF_{165}$, and promotes NRP1 internalization, which effectively shuts down receptor-mediated signaling by a second ligand.[15] This mechanism was also observed with NRP2, which shares homology to NRP1.[16]

Heparin is a sulfated polysaccharide that binds to the basic amino acid residues within the b1/b2 domain of NRP1 and enhances the binding of $VEGF_{165}$ and Sema3A to NRP1.[17] Previously, we have shown that certain sulfated polysaccharides, including dextran sulfate and Fucoidan, can bind to and reduce cell-surface levels of NRP1 by promoting the coordinate internalization of NRP1 and scavenger receptors.[18]

Endothelial cells express various scavenger receptors.[19,20] Ligands for scavenger receptors include oxidized low-density lipoprotein (LDL), acetylated LDL, maleylated bovine serum albumin (BSA), dextran sulfate, Fucoidan, and polyriboguanosine (poly G).[21,22] Scavenger receptor ligands are often polyanionic, but not all polyanions are ligands of scavenger receptors. Here, we show that synthetic poly G and oligo-deoxyriboguanosine (oligo G) bind to NRP1, induce its internalization thereby reducing its levels on the cell surface, and inhibit the binding of and biologic effects of $VEGF_{165}$ in endothelial cells. In addition, we show that intraocular administration of oligo G inhibits choroidal neovascularization (CNV) in vivo. Thus, we demonstrate that certain

---

polynucleotides or oligonucleotides act as receptor internalization inducers, promoting internalization and sequestration of critical receptors away from the cell surface and may thus have potential as therapeutic drugs.

Methods

Polysaccharides

Dextran, dextran sulfate (Mr = 500 kDa), alginic acid, carboxymethylcellulose, pectin, mannan, inulin, cellulose sulfate, carrageenan λ IV, poly-l-glutamic acid, and poly-d-glutamic acid were from Sigma-Aldrich. Cellulose sulfate was from Fisher Scientific.

Polynucleotides and oligodeoxyribonucleotides

The polyribonucleotides poly A (cat. no. P9403), poly G (cat. no. P4404), and poly C (cat. no. P4903) were purified products from ADP, GDP, and CDP, respectively (Sigma-Aldrich). The oligodeoxyribonucleotide 18-mer of deoxyadenosine (A18), deoxythymidine (T18), deoxyguanosine (G18), deoxycytidine (C18), 6-mer of deoxyguanosine (G6), phosphorothioate A18 (sA18), sT18, sG18, sC18, 5′ biotin-A18, 5′ biotin-T18, 5′ biotin-G18, 5′ biotin-C18 were custom synthesized and HPLC-purified (95%-97% purity) by Sigma Genosys (Sigma-Aldrich). Deoxyguanosine monophosphate (D9500, dGMT) was from Sigma-Aldrich.

Reagents and cytokines

Recombinant human VEGF$_{165}$, human interleukin-6 (IL-6), soluble IL-6 receptor (sIL-6R), chimeric rat NRP1/Fc, NRP2/Fc, human Sema3A/Fc, and scavenger receptor expressed by endothelial cells I (SREC-I)/Fc were from R&D Systems.

Cells and culture conditions

Primary human umbilical vein endothelial cells (HUVECs; Lonza Walkersville) were maintained in endothelial cell growth medium-2 (Lonza Walkersville).

Flow cytometric analysis

HUVECs were detached with 5mM EDTA (ethylenediaminetetraacetic acid), 1% fetal bovine serum (FBS) in phosphate-buffered saline (PBS), washed with 1% FBS buffer (PBS, 1% FBS, 10mM HEPES [N-2-hydroxyethylpiperazine-N′-2-ethanesulfonic acid]), and incubated with oligonucleotides (suspended in PBS with 1% FBS) in polypropylene round-bottom tubes at 37°C with vigorously shaking. After rinsing 2× with 1M NaCl with 0.2% BSA followed by 1% FBS buffer 2×, cells were stained with phycoerythrin (PE)-anti–BDCA-4 (NRP1) monoclonal antibody (mAb; AD5-17F6; Miltenyi Biotec), PE-anti–VEGFR-2 mAb (89 106; R&D Systems), PE-anti–VEGFR-1 mAb (49 560; R&D Systems), fluorescein isothiocyanate (FITC)-anti–CD31 mAb (WM59; BD Biosciences), anti-NRP2 mAb (C-9; Santa Cruz Biotechnology), anti-gp130 mAb (AM64; BD Biosciences), or anti–SREC-I Ab (AF2409; R&D Systems) followed by Alexa 488–conjugated anti–mouse Ab or Alexa 488–conjugated anti–goat Ab (Invitrogen). Data were collected using a FACSCalibur cytofluorometer (BD Biosciences).

Laser confocal microscopy

Endothelial cells growing onto glass chamber slides (Nalge Nunc International) coated with 5 µg/mL fibronectin were incubated (37°C, 5% CO$_2$) with sG18 (in 1% FBS buffer) with protease inhibitor cocktail (Nacalai Tesque) for 15 or 60 minutes. The medium was replaced with 4% (wt/vol) paraformaldehyde (PFA) for fixation, and cells were washed with PBS and permeabilized with 0.1% Triton X-100 in PBS. Cells were then stained with Alexa Fluor 488– or 546–conjugated streptavidin (Invitrogen), mouse anti–human NRP1 mAb, goat anti–human SREC-I Ab, rabbit anti–human lysosome-associated membrane protein-2 (LAMP2) Ab (Abcam), or rabbit anti-phospho VEGFR-2 (Y1175) mAb (19A10; Cell Signaling

Technology) in PBS with 3% BSA and 3% FBS at 4°C for 16 hours. After washing with PBS, slides were incubated with Alexa 488–conjugated anti–mouse IgG Ab, Alexa Fluor 594-conjugated anti–rabbit IgG Ab or Alexa 594–conjugated anti–goat immunoglobulin G (IgG) Ab (Invitrogen), washed, and mounted with VECTASHIELD with DAPI (4′,6-diamidino-2-phenylindole; Vector Laboratories). Images were obtained using the LSM 510 Zeiss confocal microscope (Carl Zeiss MicroImaging).

Surface plasmon resonance

Biotin-G18 was injected onto the flow cell of the Sensor Chip SA (Biacore), which is coated with streptavidin; 940 resonance units (RUs) of biotin-G18 were immobilized onto the streptavidin-coated chip. The flow cell was then conditioned with several injections of 2M NaCl. NRP1-G18-binding assay was performed by surface plasmon resonance using a Biacore 2000 system (Biacore). NRP1/Fc chimera was diluted in HEPES buffer saline containing 0.005% Surfactant P20 (HBS-P; Biacore) maintained at 25°C and injected over the G18-coated or control flow cell surfaces at a flow rate of 50 µL/minute. Association and dissociation phases were evaluated over 2 minutes, respectively. To evaluate the dissociation phase, the complexes that formed were washed with HBS-P at a flow rate of 50 µL/min over 2 minutes. Sensor chips were regenerated with 2 pulses of 2M NaCl for 1 minute. Kinetic constants were obtained from the sensorgrams using BIAevaluation software (Biacore). Dissociation constant (Kd) was calculated from the ratio of dissociation and association rate constants (Kd = k_{off}/k_{on}).

Enzyme-linked immunosorbent assay–based binding assays

Flat-bottom microtiter plates (96-well Immulon 4HBX; Thermo Labsystems) were coated with BSA, human IgG1 (Merck), NRP1/Fc, or NRP2/Fc (2 µg/mL). After blocking with PBS containing 0.1% Tween 20 and 5% BSA, biotin-G18 (4 µg/mL in PBS with 0.1% Tween 20 and 1% BSA) was added. Bound biotin-G18 was detected by streptavidin-horseradish peroxidase (HRP; GE Healthcare). Coated IgG1, NRP1/Fc, and NRP2/Fc proteins were detected by anti-human IgG-HRP (GE Healthcare). Binding of biotin-oligos to NRP1 was examined as follows: after blocking (PBS containing 0.1% Tween 20 and 5% BSA) the wells precoated with NRP1/Fc or with SREC-I/Fc chimeric proteins (all at 2 µg/mL), biotin-A18, -T18, -G18, or -C18 (0.25, 1, 4, 16 µg/mL in PBS, 0.1% Tween 20, 1% BSA) was added. Bound biotin-oligo was detected by streptavidin-HRP. Binding of NRP1/Fc to SREC-I/Fc was examined by addition of His-tagged NRP1/Fc with or without biotin-A18, -T18, -G18, or -C18 (0.25, 1, 4, 16 µg/mL) onto SREC-I–coated wells. Bound NRP1/Fc was detected by anti-His mAb (Invitrogen), followed by HRP-conjugated anti–mouse IgG Ab (GE Healthcare). Reactions were visualized with tetramethoxybenzene peroxidase substrate (KPL) followed by addition of 1M H$_2$SO$_4$, and read at 450 nm.

Western blotting

After endothelial cell incubation (in PBS containing 1% FBS) with or without 16 µg/mL sG18, the cells were stimulated with VEGF$_{165}$ (100 ng/mL) or IL-6 (100 ng/mL) plus sIL-6R (100 ng/mL) for 5 minutes. The cells were lysed in lysis buffer [1% sodium dodecyl sulfate (SDS), 150 mM NaCl, 10 mM Tris-HCl, pH 7.4] with phosphatase inhibitor cocktail and protease inhibitor cocktail (Nacalai Tesque). Cell lysates were separated by SDS–polyacrylamide gel electrophoresis (SDS-PAGE), transferred onto nitrocellulose membranes, and immunostained using rabbit mAb to phosphorylated human VEGFR-2 (Tyr1175) or rabbit mAb to phosphorylated human STAT3 (Tyr705; both from Cell Signaling Technologies), followed by incubation with an HRP-conjugated anti–rabbit IgG antibody (GE Healthcare). Immunocomplexes were visualized with a chemiluminescence detection system. After stripping the immunocomplexes with stripping solution (Nacalai Tesque), the membranes were reblotted with rabbit anti–VEGFR-2 or rabbit anti-STAT3 Abs (both from Santa Cruz Biotechnology).

Endothelial cell transmigration assay

Endothelial cell migration assays were performed using 0.2% gelatin-coated polycarbonate transwell filters (pore size 8 µm; Costar). After

preincubation at 37°C for 30 minutes with sG18 or sA18 (0-16 μg/mL), HUVECs were suspended in migration medium (RPMI1640 with 0.5% BSA and 10mM HEPES), and placed in the upper chamber. The lower chamber contained medium only or with VEGF$_{165}$ (50 ng/mL). After an 18-hour incubation at 37°C, viable cells in the lower chamber were counted.

Endothelial cell proliferation assay

HUVECs (5000 cells/well) were cultured for 24 hours in 96-well tissue culture plates (Corning) in DMEM supplemented with 10% FBS and 2 μg/mL heparin, with or without 25 ng/mL VEGF$_{165}$ in the presence of sA18, sT18, sG18, or sC18 (0, 1, 2, 4, 8, 16, or 32 μg/mL). Cell proliferation was measured by using Cell Counting Kit-8 (Dojindo).

Laser-induced CNV

All mouse protocols were approved by the appropriate National Institutes of Health (NIH) animal care and use committee and were conducted according to the approved protocol. The technique was carried out essentially as described.[23] Ten-week–old female C57BL6 mice (Frederick, MD) were anesthetized, and the pupils were dilated. After positioning on a rack connected to a slit lamp system, 4 photocoagulation spots (75 μm size, 75 ms, 90 mW power) were made in each eye at approximately equal distance from the optic nerve with the Oculight infrared laser system (810 nm; IRIDEX Corporation). The targeted sites were visualized through a hand-held lens and a viscous surface lubricant. Only lesions resulting in formation of a bubble at the time of laser treatment were used for further evaluation. Compounds (sA18 or sG18) diluted in vehicle (saline) or vehicle alone were injected at different concentrations once in a total volume of 1μL into the vitreous immediately after laser treatment. As a positive control, we used the neutralizing anti-VEGF-A mAb B20.4.1,[11] the anti-NRP1^B mAb[11] (both antibodies a gift of Genentech), or a corresponding IgG at the concentration of 2 μg/μL (total injection volume 1 μL/eye). After laser treatment, the mice were given a lubricant ophthalmic ointment treatment. One week after laser treatment, the choroids were isolated and stained with Alexa Fluor 594-conjugated isolectin B4 (IB4), as directed by the manufacturer (Invitrogen). After IB4 staining, the eyecups were flat-mounted in Aquamount with the sclera facing down. The total neovascular area stained with IB4 was measured using Axiovision software (Carl Zeiss). The mean neovascular area/eye was calculated from the measurements of the individual lesions. Sections were also stained with hematoxylin and eosin (H&E; HistoServ). For immunocytochemistry, the eyes were fixed in 4% PFA in PBS for 18 hours at 4°C, embedded in OCT, and immediately frozen and sectioned (5-μm sections). Before staining, slides were postfixed in cold 4% PFA in PBS for 5 minutes and washed twice for 10 minutes in PBS. Slides were blocked in 3% goat serum, 1% BSA, 0.3% Triton X-100 in PBS (for 1 hour at room temperature), and then incubated overnight at 4°C with primary antibodies: rat anti-mouse CD31 (Becton Dickinson), human anti-mouse NRP1^B (11 a gift of Genentech), and rat anti-mouse F4/80 (Caltag). The slides were washed twice with 1% Triton X-100 in PBS, and secondary antibodies goat anti-mouse Alexa Fluor 647, goat anti-human Alexa Fluor 488 (Molecular Probes, Invitrogen), and DAPI (for detection of nuclei) were added for 1 hour at room temperature. After 2 washes with PBS-Triton, slides were mounted and observed through an Axiovert 200 fluorescence microscope (Carl Zeiss) using optimized excitation/emission filter sets (Omega Optical). The images were digitalized using Volocity imaging program (Improvision), the pseudocolored images were converted into tiff files, exported into Photoshop (Adobe Systems) and overlaid as individual layers to generate merged composites. Images were processed with Adobe Photoshop. Infiltration with monocyte/macrophages was evaluated by digital measurement (ImageJ software) of F4/80$^+$cells within injured areas. The results are expressed as the mean monocyte/macrophage infiltration/injured area.

Statistical analysis

Group means, standard deviations (SD), standard errors of the mean (SEM), and significance of differences between group means (2-tailed Student t test) were calculated. P values less than .05 are considered significant.

Results

Effects of poly G and oligo G on cell surface of NRP1

Previously, we reported that certain scavenger receptors ligands, including dextran sulfate and Fucoidan, reduce NRP1 levels on the cell surface.[18] We now examined whether other sulfated polysaccharides can modulate cell-surface levels of NRP1. Cellulose sulfate and carrageenan also reduced cell-surface levels of NRP1, but not alginic acid, carboxymethylcellulose, pectin, mannan, inulin, poly-l-glutamic acid, and poly-d-glutamic acid (Figure 1A). As expected,[18] sulfated polysaccharides reduced cell-surface levels of NRP1, but not nonsulfated polysaccharides. The polysaccharides that reduced cell-surface levels of NRP1 are cationic molecules known to be ligands for scavenger receptors.[21,22] Poly G is also known to be a ligand for scavenger receptors.[24] As shown in Figure 1B, we found that poly G reduces cell-surface levels of NRP1, whereas poly A and poly C, not known to be scavenger receptor ligands, do not. We also examined the effects of oligo G oligonucleotides on NRP1 surface levels. As shown in Figure 1B, an 18-mer of G (G18) dose-dependently reduced cell-surface levels of NRP1, whereas A18, T18, and C18 did not. Phosphorothioate oligo G (sG18) also dose-dependently reduced cell-surface NRP1 levels, indicating that the phosphorothioate modification did not compromise the ability of oligo G to reduce cell-surface levels of NRP1. Oligo G comprising 6 G residues (G6) also reduced NRP1, whereas a single G (sGMT) did not (Figure 1B). Reduction of cell-surface NRP1 in HUVECs could not be attributed to pH-related toxicity, as all solutions containing G18, sG18, or G6 were at pH 7.4. Acetylated LDL, a ligand for scavenger receptors,[21,22] did not reduce cell-surface levels of NRP1 (data not shown), indicating that scavenger receptor ligand alone is insufficient for reduction of cell-surface levels of NRP1.

We examined oligo and poly G selectively for NRP1. As shown in Figure 2A, G18 minimally altered cell-surface levels of NRP2, VEGFR-2, VEGFR-1, gp130, or CD31, but reduced those of SREC-I, indicating that G18 does not indiscriminately alter detection of cell-surface molecules. Similar results were derived with poly G (not shown). We examined the conditions for reduction of cell-surface NRP1. G18 time-dependently reduced cell-surface NRP1 at 37°C over 60 minutes, but was less effective and slower at reducing cell-surface NRP1 at 4°C (Figure 2B). To examine the effects of G18 in serum, we used phosphorothioate oligonucleotides, which are stable in medium containing high concentrations of serum. As shown in Figure 2C, sG18 dose-dependently reduced levels of endothelial cell-surface NRP1 in the presence of 95% FBS, albeit to a somewhat lower degree and at higher concentrations than in the presence of 1% FBS. Thus, G18 dose-dependently reduces cell-surface NRP1 in endothelial cells even in the presence of a high serum concentration.

G18 promotes the internalization of cell-surface NRP1

We next examined whether G18 can promote the internalization of NRP1, thus explaining its reduction on the cell surface after incubation with G18. Using confocal microscopy, we traced NRP1 in endothelial cells after incubation with sG18 (Figure 3A). NRP1 is minimally detectable by confocal microscopy (1-μm slice cuts) in cultured endothelial cells that have been fixed and permeabilized as it is diffusely distributed.[15] However, NRP1 was clearly detectable at the endothelial-cell rim and only partially inside the cytoplasm after 15 minutes incubation with sG18 (16 μg/mL at
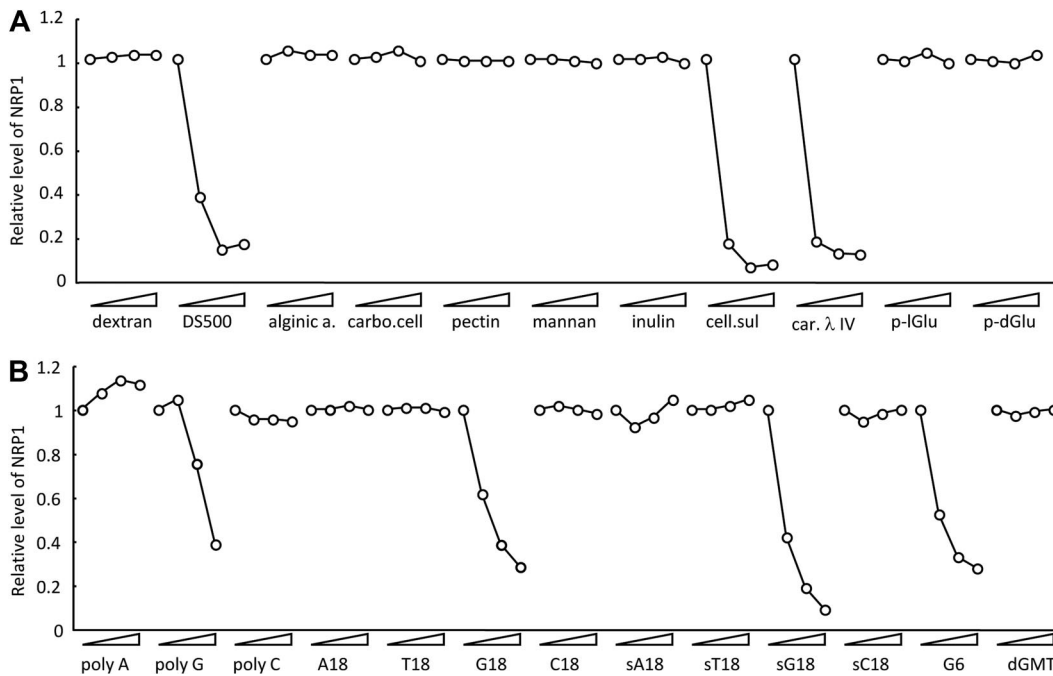
Figure 1. Modulation of cell-surface NRP1 by polysaccharides and poly- and oligonucleotides. HUVECs were incubated at 37°C for 1 hour with the indicated compounds (each tested at 0, 1, 8, 64 μg/mL); after incubation, NRP1 was detected by flow cytometry. Compounds tested in (A) dextran, 500-kDa dextran sulfate (DS500), alginic acid (alginic a.), carboxymethylcellulose (carbo. cell), pectin, mannan, inulin, cellulose sulfate (cell. sul), carrageenan λ IV (car. λ IV), poly-l-Glu acid (p-lGlu), and poly-d-Glu acid (p-dGlu); in (B) polyribonucleotides poly A, poly G, and poly C; oligodeoxyribonucleotides T18, G18, C18, G6; phosphorothioate oligodeoxyribonucleotides sA18, sT18, sG18, sC18, and dGMT. Results reflect the relative mean fluorescence intensities with and without compounds.

37°C). After 60 minutes incubation with sG18, NRP1 was detectable almost exclusively inside the cytoplasm including the perinuclear region. Thus, in the presence of sG18, cell-surface NRP1 levels are decreased as measured by flow cytometry, and the location of NRP1 changes from the cell-surface rim to inside the cytoplasm as detected by confocal microscopy. The delay in NRP1

internalization detected by confocal microscopy (Figure 3A) as opposed to flow cytometry (Figure 2B) is likely attributable to the differences in experimental conditions.

We examined the location of G18 and NRP1 relative to each other. After incubation with biotin-labeled G18 (16 μg/mL) at 37°C for 60 minutes, double-staining for NRP1 and biotin-G18
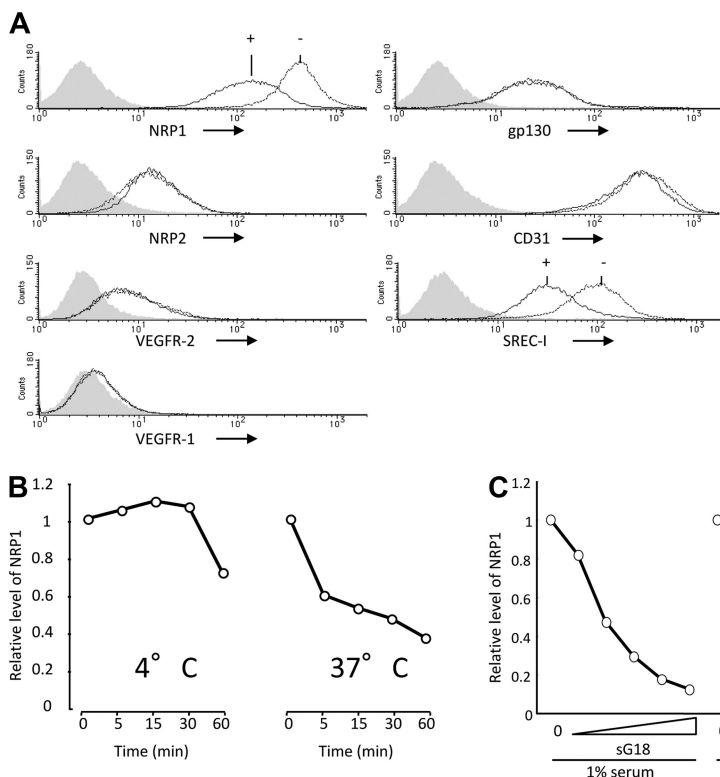

Figure 2. Selective reduction of NRP1 by G18 is temperature-dependent. (A) Effects of G18 on levels of cell-surface NRP1, NRP2, VEGFR-2, VEGFR1, gp130, CD31, and SREC-I detected by flow cytometry. HUVECs were incubated at 37°C for 1 hour with or without G18 (16 μg/mL). Shaded graphs reflect control staining. (B) Temperature- and time-dependent reduction of cell-surface NRP1 by G18. HUVECs were incubated with G18 (16 μg/mL) at 4° or 37°C for 5, 15, 30, and 60 minutes. The results reflect the relative mean fluorescence intensities of NRP1 under the conditions of testing. (C) Levels of cell-surface NRP1 detected by flow cytometry on HUVECs incubated with sG18 (0, 1, 2, 4, 8, or 16 μg/mL) in the presence of 1% FBS or with sG18 (0, 4, 8, 16, 32, or 64 μg/mL) in the presence of 95% FBS.
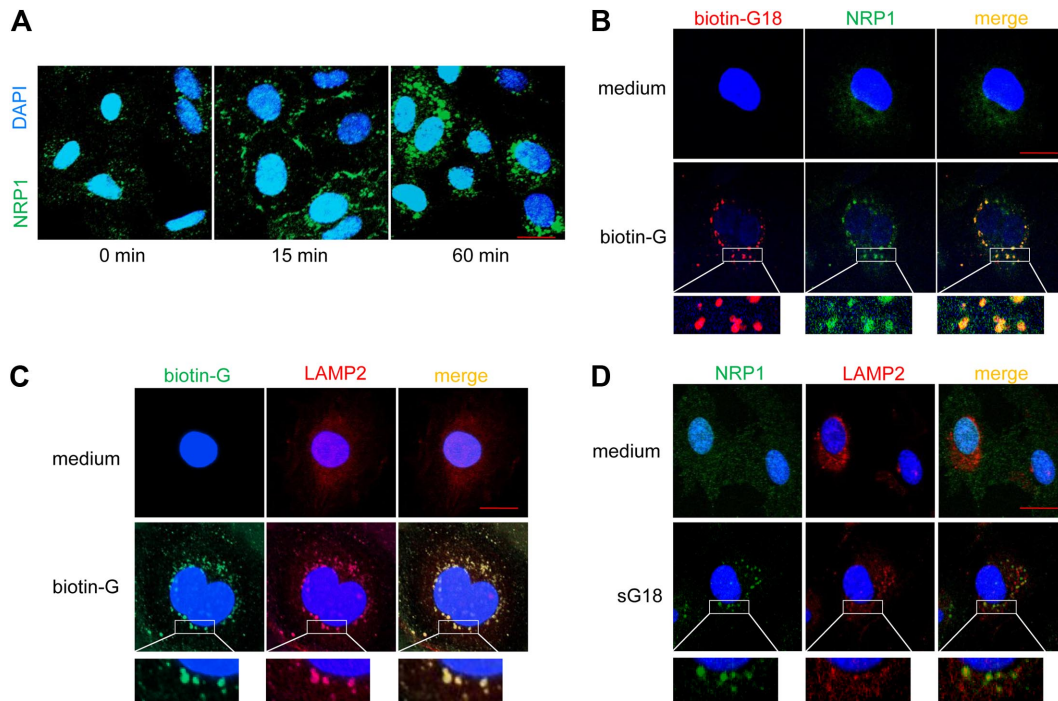
Figure 3. G18 promotes internalization of NRP1 and associates with NRP1 in LAMP2-marked structures. (A) Cells were incubated in medium alone or with 16 μg/mL sG16 at 37°C for 15 and 60 minutes. After fixation and permeabilization, cells were stained with anti-NRP1 primary mAb followed by Alexa 488–conjugated anti–mouse IgG Ab. Nuclei were stained with DAPI. (B) Cells were incubated with medium alone (top panels) or 16 μg/mL biotin-G18 (bottom panels) at 37°C for 60 minutes. After fixation and permeabilization, cells were stained with Alexa Fluor 546–conjugated streptavidin (to visualize biotin-G18) and with anti-NRP1 primary mAb followed by Alexa Fluor 488–conjugated anti–mouse IgG Ab (to visualize NRP1). (C) Cells were incubated with medium only (top panels) or 16 μg/mL biotin-G18 (bottom panels) at 37°C for 60 minutes. After fixation and permeabilization, cells were stained with Alexa Fluor 488–conjugated streptavidin (to visualize biotin-G18) and with anti-LAMP2 primary Ab followed by Alexa Fluor 594–conjugated anti–rabbit IgG Ab (to visualize LAMP2). (D) Cells were incubated with medium only (top panels) or 16 μg/mL sG18 (bottom panels) at 37°C for 60 minutes. After fixation and permeabilization, cells were stained with anti-NRP1 primary mAb followed by Alexa Fluor 488–conjugated anti–mouse IgG Ab (to visualize NRP1) and with anti-LAMP2 primary Ab followed by Alexa Fluor 594–conjugated anti–rabbit IgG Ab (to visualize LAMP2). Cells were examined by confocal microscopy. Images were imported into Adobe Photoshop 6.0 for processing. Scale bar, 20 μm.

showed that the 2 molecules colocalize in vesicular cytoplasmic structures (Figure 3B, lower panels). Together, these results provide evidence that G18 promotes NRP1 internalization and associates with NRP1. The vesicular structures containing biotin-G18 (Figure 3C) and NRP-1 (Figure 3D) costained for LAMP2, indicative of lysosomal localization of the internalized NRP-1.

Analysis of oligo G binding to NRP1

Because oligo G selectively reduces cell-surface levels of NRP1, promotes NRP1 internalization, and colocalizes with NRP1 in the cytoplasm, it could directly bind to NRP1. We tested this possibility using enzyme-linked immunosorbent assay (ELISA)–based assays. BSA, IgG1, NRP1/Fc, or NRP2/Fc were first immobilized onto the well, and then biotin-G18 (4 μg/mL) was added. The bound biotin-G18 was detected by streptavidin-HRP. As shown in Figure 4A top, we found that biotin-G18 binds to NRP1 and to a much lower degree to NRP2. Reduced biotin-G18 binding to NRP2 compared with NRP1 could not be attributed to uneven coating (Figure 4A bottom). In additional assays, NRP1/Fc was first immobilized onto the well, and then biotin-A18, biotin-T18, biotin-G18, and biotin-C18 were added at varying concentrations. The bound biotin-oligonucleotides were detected by streptavidin-HRP. As shown in Figure 4B, we found that biotin-G18 bound to NRP1, but biotin-A18 and biotin-T18 did not, and that biotin-C18 bound to NRP1 to a lower degree. We further examined the specificity of biotin-G18 binding to NRP1 by adding excess unlabeled G18, A18, T18, or C18 to wells in which biotin-G18 was added onto the NRP1-coated wells. As shown in Figure 4C, only unlabeled G18 inhibited the binding of biotin-G18 to NRP1,

indicating that guanosine residues are critical to the binding of biotin-G18 to NRP1. Using surface plasmon resonance (Biacore system), we confirmed that recombinant NRP1 extracellular domain dose-dependently binds to a G18-coated sensor chip (Figure 4D). On the basis of the results of 3 experiments, the Kd for the NRP1-G18 interaction was calculated at 1.3 ± 0.16nM [association rate constant (ka) $2.9 \pm 0.84 \times 10^6$ 1/Ms and dissociation rate constant (kd) $3.7 \pm 0.72 \times 10^{-3}$ 1/s]. Control BSA or human IgG1 did not bind to a G18-coated sensor chip (not shown).

In additional experiments, we tested whether oligo G can directly bind to SREC-I, as this would explain why oligo G reduces cell-surface levels of SREC-I. To this end, we used an ELISA-based assay in which SREC-I/Fc is immobilized onto the well, and biotin-A18, biotin-T18, biotin-G18, and biotin-C18 are then added at varying concentrations; the bound biotin-oligonucleotides are detected by streptavidin-HRP. As shown in Figure 4E, we found that biotin-G18 binds to SREC-I, but biotin-A18, biotin-T18, and biotin-C18 do not.

Because we had found that G18 binds to NRP1 and SREC-I, we tested whether G18 can simultaneously bind both molecules, thereby bridging together SREC-I and NRP1. To this end, we used an ELISA-based assay in which SREC-I/Fc is immobilized onto a well and NRP1/Fc is subsequently added with or without biotin-oligonucleotides. As shown in Figure 4F, we found that biotin-G18 dose-dependently promotes the binding of NRP1 to SREC-I, providing evidence that G18 can serve to bridge together NRP1 and SREC-1 at least in a cell-free system.

In additional experiments, we tested whether G18 has an ability to bridge together NRP1 and SREC-I in endothelial cells, as these
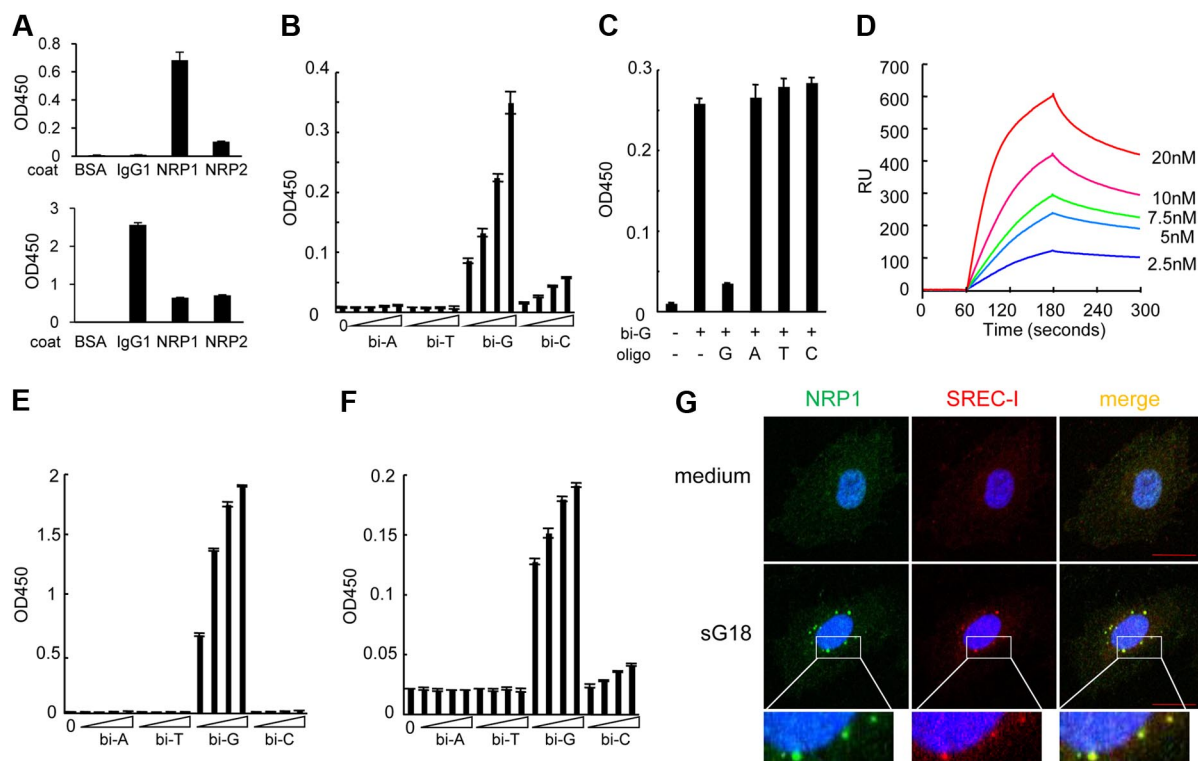
Figure 4. Characterization and functional consequences of G18 binding to NRP1 and SREC-I. (A) Analysis of biotin-G18 binding to NRP1-Fc and NRP2-Fc. Top panel, binding of biotin-G18 to BSA-, IgG1-, NRP1-, or NRP2-coated wells detected by ELISA-based measurement of streptavidin-HRP. Bottom panel, detection of coated proteins by anti-IgG1 antibody detected by ELISA. The results reflect the means ± SD of triplicate wells. (B) Binding of biotin-G18 to NRP1. Biotin-A18, -T18, -G18, or -C18 (0.25, 1, 4, 16 μg/mL) was added to NRP1-coated wells. Bound biotin-olionucleotides were detected by ELISA-based measurement of streptavidin-HRP. The results reflect the means ± SD of 3 experiments. (C) Biotin-G18 binding to NRP1 is selectively blocked by nonbiotin-G18. Biotin-G18 (1 μg/mL) was added to NRP1-coated wells in the presence of G18, A18, T18, or C18 (100 μg/mL). (D) Characterization of NRP1 binding to immobilized G18. Plasmon resonance (Biacore)-generated sensorgrams showing a kinetic analysis of NRP1 binding to G18. Biotin-G18 was immobilized onto the sensor chip. NRP1/Fc (2.5, 5, 7.5, 10, or 20nM) was passed over the sensor surface. Representative results from 4 independent experiments are shown. (E) Binding of biotin-G18 to SREC-I. Biotin-A18, -T18, -G18, or -C18 (0.25, 1, 4, or 16 μg/mL) was added to SREC-I–coated wells. Bound biotin-olionucleotides were detected by ELISA-based measurement of streptavidin-HRP. The results reflect the means ± SD of 3 experiments. (F) G18 bridges NRP1 to SREC-I. His-tagged NRP1/Fc (1 μg/mL) was added to SREC-I/Fc-coated wells in the presence of A18, T18, G18, or C18 (0, 0.25, 1, 4, or 16 μg/mL). Bound His-tagged NRP1/Fc was detected by HRP-conjugated anti-His Ab. The results reflect the means ± SD of 3 experiments. (G) G18 induces the coordinate internalization of NRP1 and SREC-I. HUVECs were incubated with or without sG18 (16 μg/mL at 37°C for 1 hour). After fixation and permeabilization, cells were stained with anti-NRP1 mAb (green), anti-SREC-I Ab (red), and DAPI (blue) and were examined by confocal microscopy. Top panels are from cells incubated in medium alone; bottom panels are from cells incubated with sG18. Scale bar, 20 μm.

cells express both NRP1 and the scavenger receptor SREC-I. The presence of G18-induced bridging would be reflected by NRP1 and SREC-I colocalization in endothelial cells. Using confocal microscopy, we found that in the presence of G18, NRP1 and SREC-I colocalize within endothelial cells that have been incubated with G18 for 60 minutes, but not in medium only without G18 (Figure 4G). We determined that 88% of NRP1-staining vesicles costained for SREC-I (we counted 84 vesicles from 10 randomly selected cells). Thus, G18 can bridge NRP1 to SREC-I and promote their internalization in endothelial cells.

G18 blocks VEGF$_{165}$ function in endothelial cells

We examined the potential functional significance of surface NRP1 reduction by G18. Pretreatment of endothelial cells with sG18 (at 0, 4, 16 μg/mL for 1 hour), followed by cell washing, dose-dependently reduced the binding of VEGF$_{165}$ and Sema3A to the cell surface (Figure 5A). Instead, pretreatment with sA18, sT18, and sC18 (all at 16 μg/mL) minimally affected the binding of VEGF$_{165}$ and Sema3A to HUVECs (data not shown). To test this further, we examined the effects of oligonucleotides on VEGF$_{165}$-induced signaling, migration, and proliferation of endothelial cells. As shown in Figure 5B and C (immunoblotting results and confocal microscopy), sG18 specifically inhibited the phosphorylation of VEGFR-2 induced by VEGF$_{165}$. As expected from

reduced phosphorylation of VEGFR-2, sG18 also inhibited Erk1/2 phosphorylation induced by VEGF$_{165}$ (not shown). By contrast, sG18 did not inhibit the phosphorylation of STAT3-induced IL-6 in conjunction with sIL-6R (Figure 5B). In functional studies, sG18, but not sA18, markedly inhibited the migration (Figure 5D) and proliferation (Figure 5E) of HUVECs in response to VEGF$_{165}$. By contrast, sG18 reduced bFGF-induced HUVEC proliferation by only approximately 40% at 16 μg/mL (not shown). Thus, G18 reduces endothelial cell-surface levels of the VEGF$_{165}$ coreceptor NRP1, VEGF$_{165}$ binding to endothelial cells, and VEGF$_{165}$-induced signaling, migration, and proliferation in endothelial cells.

G18 inhibits CNV in vivo

We next used a laser-induced CNV mouse model to evaluate the antiangiogenic activity of G18, as intravitreal administration of other antiangiogenic compounds detected antiangiogenic activity in this model.[25] The laser-induced CNV model is a commonly used disease model for neovascular age-related macular degeneration (AMD), which is a major cause of blindness in aged individuals in Western societies. Four laser spots were introduced into the choroid of each eye (schematic representation, Figure 6A left) to produce localized disruption of the choroidal layer and the Bruch membrane, as visualized in a representative image from H&E staining

Figure 5. sG18 inhibits VEGF$_{165}$ and Sema3A binding to HUVECs and VEGF$_{165}$-induced HUVEC proliferation. (A) sG18 inhibits VEGF$_{165}$ and Sema3A binding to HUVECs. The cells were incubated with sG18 (0, 4, or 16 μg/mL) at 37°C for 1 hour, followed by addition of biotin-VEGF$_{165}$ or Sema3A/Fc. Bound biotin-VEGF$_{165}$ or Sema3A/Fc was detected by flow cytometry. (B) sG18 (16 μg/mL) inhibits VEGF$_{165}$-induced phosphorylation of VEGFR-2 in HUVECs. After incubation with sG18 (0 or 16 μg/mL) at 37°C for 1 hour, the cells were treated with VEGF$_{165}$ (100 ng/mL) or IL-6 (100 ng/mL) in conjunction with sIL-6R (100 ng/mL) at 37°C for 5 minutes. Phosphorylated (p-Y) VEGFR-2 and p-Y STAT3 was detected by immunoblotting with specific antibodies; after stripping, the membranes were reprobed for total VEGFR-2 and STAT3. Molecular weights (kDa) are indicated on the left of the panel. (C) sG18 inhibits VEGF$_{165}$-induced phosphorylation of VEGFR-2 in HUVECs, as detected by confocal microscopy. Conditions for cell incubation with sG18 and VEGF$_{165}$-induced activation of VEGFR-2 are those described in panel B. (D) sG 18 specifically inhibits VEGF$_{165}$ (50 ng/mL)-induced transwell migration of endothelial cells. HUVECs (5 × 10^5 cells/well) were preincubated for 30 minutes with sG18 or sA18 (1, 4, or 16 μg/mL) added to the upper chamber and incubated at 37°C for 18 hours. The results reflect the mean fold increase (± SEM) in cell migration compared with medium alone in 3 experiments performed in duplicate. (E) HUVECs were cultured for 24 hours with or without sA18, sT18, sG18, or sC18 at varying concentrations (1, 2, 4, 8, 16, or 32 μg/mL) in the presence of VEGF$_{165}$ (25 ng/mL); proliferation was measured by Cell Counting Kit-8. Results are expressed as mean ± SD optical density at 450 nm of triplicate cultures.
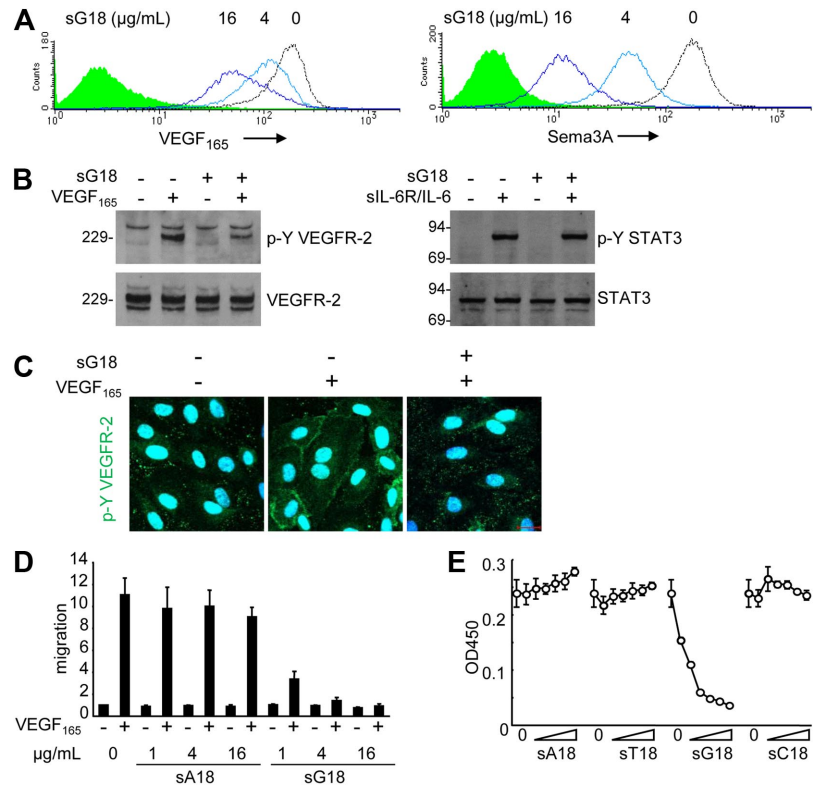
(Figure 6A right). Laser injury of the choroid induces local choroids neovascularization, VEGF production, and recruitment of monocyte/macrophages to the lesions.[23,25,26] We tested whether G18 is antiangiogenic in this model by inoculating sG18 in the vitreous body of each eye immediately after imparting laser delivery. Groups of 7 mice received the oligonucleotides (sG18 or sA18) once at different concentrations (1, 3, and 10 μg/eye; total injection volume 1 μL) or vehicle (saline) alone (1 μL). After 7 days, the eyes were removed, and the degree of neovascularization within the laser-injured areas evaluated. As shown in representative images (Figure 6B), CD31 immunostaining was more prominent in the CNV areas of eyes treated with sA18 compared with those treated with sG18, likely reflecting the inhibition of CNV by sG18. Instead, NRP1 immunostaining failed to detect
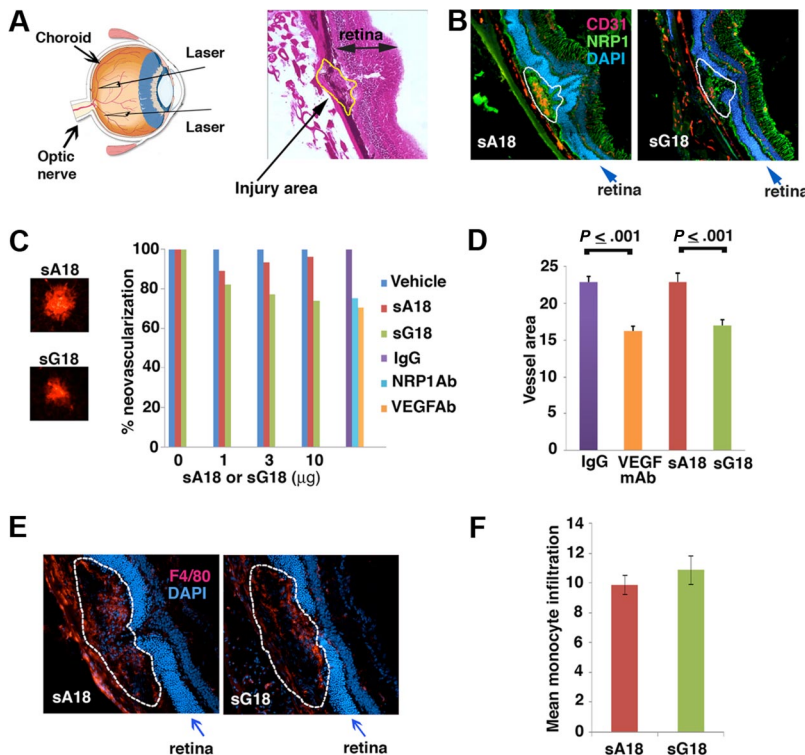

Figure 6. sG18 inhibits CNV induced by laser injury. (A) Laser injury to the choroids and Bruch membrane. Left panel, schematic representation of the procedure. Right panel, representative image depicting a typical area of CNV (denoted by the dotted line); H&E staining. (B) Representative images from immunostaining of CNVs 7 days after laser injury and treatment with sA18 or sG18; CD31 (red) and NRP1 (green); nuclei are visualized by DAPI (blue). The dotted line denotes the CNV areas. (C) Analysis of CNV detected by Alexa Fluor 594–labeled isolectin B4 (IB4) staining. Left, representative images from IB4 staining of CNV spots treated with sA18 and sG18. Right, quantitative analysis of CNV. Eyes were removed 7 days after laser injury and treatment with vehicle alone or with the indicated additives. Mean area of CNV was first measured for each mouse (4 injured areas/eye). The results reflect group means (7 mice/group) and are expressed as percent mean neovascular area compared with vehicle alone. (D) VEGF neutralizing antibody and sG18 reduce CNV after laser injury. The results reflect quantitative measurement of neovascular areas stained by Alexa Fluor 568-labeled IB4 and reflect group means ± SEM. Groups of 7 mice were treated with neutralizing antibody to human/mouse VEGF (B20.4.1, 2μg/eye), sG18 (10 μg/eye), and appropriate controls; the eyes were removed 7 days after injury. (E) Representative images depicting monocyte/macrophage infiltration of CNV areas (denoted by the dotted line) detected by immunostaining with antibodies to the monocyte/macrophage marker F4/80 (red); nuclei are stained with DAPI (blue). Eyes were removed 7 days after laser injury and treatment with sA18 or sG18. (F) Quantitative analysis of monocyte/macrophage infiltration in CNV areas detected by immunostaining with F4/80 antibodies and analysis (ImageJ). The results are expressed as group means ± SEM. Each group consisted of 5 mice treated in the eye with sA18 or sG18.

clear differences between sA18- and sG18-treated eyes, likely reflecting the wide distribution of NRP1 expression in the retinas and CNVs (Figure 6B). For quantitative analysis of neovascularization, choroidal whole mounts stained with Alexa Fluor 594–labeled isolectin B4 (IB4) were evaluated. Representative images from IB4 staining of CNV spots treated with sA18 or sG18 are shown in Figure 6C left. We found that sG18 dose-dependently reduced CNV, whereas sA18 was minimally effective compared with vehicle only (Figure 6C right). At the highest dose (10 μg/eye), sG18 significantly reduced CNV compared with sA18 (Figure 6D). The degree of angiogenesis inhibition by sG18 (26%) was comparable in magnitude ($P > .05$) to that achieved by the intravitreal administration of neutralizing antibodies to NRP1 or VEGF-A used at optimal concentrations (2 μg/eye) in parallel experiments (Figure 6C-D).

Recruitment of monocyte/macrophages is known to accompany CNV after laser delivery and may contribute to angiogenesis through monocyte-derived proangiogenic molecules.[25,26] We examined whether sG18 reduces choroidal angiogenesis at least in part by reducing choroidal inflammation with monocyte/macrophages. Immunostaining for the monocyte/macrophage–specific marker F4/80 showed clear infiltration with monocye/macrophages (representative images from eyes treated with sA18 and sG18 are shown in Figure 6E), but detected no significant difference ($P > .05$) in the levels of monocyte/macrophage infiltration within the CNVs treated with sG18 or sA18 (Figure 6F). Overall, these results provide evidence that sG18 is antiangiogenic in an in vivo model of CNV.

Discussion

We demonstrate that poly G and oligo G reduce endothelial cell-surface NRP1, thereby inhibiting the binding, signaling, and function of VEGF$_{165}$ and provide evidence for the mechanism underlying these effects. In brief, oligo G binds to NRP1, bridges the extracellular domain of NRP1 to that of the scavenger receptor SREC-I, and promotes their coordinate internalization and trafficking to the lysosome. We also show that local injection of oligo G into the eye inhibits CNV in vivo as effectively as anti-VEGF Ab. These results provide evidence that synthetic G oligonucleotides are internalization inducers of NRP1 in endothelial cells and antiangiogenic molecules.

Several strategies for functional inhibition of cell-surface receptors have been explored. One strategy is to use competitive blockers competing with natural ligands for binding to target receptors through higher receptor affinity or higher concentration than the natural ligand; this includes neutralizing antibodies, such as the IL-6 receptor antibody[27] or small compound receptor antagonists, such as histamine receptor blockers. Another strategy is the induction of receptor internalization with internalization inducers.[18,28] Two such internalization inducers, dextran sulfate and Fucoidan,[18] are effective at blocking target molecules, because they induce the sequestration of receptors inside the cells away from their surface ligands, without themselves promoting receptor signaling. Interestingly, internalization inducers need not display higher affinity than the natural ligands.

NRP1 internalization and the associated reduction of VEGF-A responses likely contribute to the antiangiogenic activity of oligo G in the laser-induced CNV model. Consistent with these results, other studies have shown that NRP1 neutralization inhibited VEGF$_{165}$ binding to endothelial cells and reduced pathologic

angiogenesis in vivo.[11] However, we cannot exclude the participation of other mechanisms. Reduction of cell-surface NRP1 itself by oligo G may impair endothelial cell attachment and angiogenesis, independently of VEGF.[29,30] In addition, oligo G may functionally alter receptors/factors not tested here. Phosphorothioate oligos of cytidine and thymidine were reported to bind platelet-derived growth factor (PDGF) and inhibit its function, which could reduce angiogenesis.[31] G-rich oligonucleotides inhibited expression of STAT3, hypoxia-inducible factor-1 α (HIF-1α), and HIF-2α, critical transcription factors in angiogenesis.[32-35] Recently, myeloid cells, including macrophages, were found to contribute to pathologic angiogenesis[36] through secretion of MMP-2, MMP-9, and Bv8/prokineticin-2.[36,37] Monocytes/macrophages are recruited to sites of neovascularization in the choroidal laser-injury model analyzed here and likely contribute to angiogenesis.[25,26] Although our analysis found that sG18 did not decrease levels of monocyte infiltration after choroidal injury, we cannot exclude that sG18 may functionally inactivate proangiogenic factors produced by monocyte/ macrophages at this site. Interestingly, G-rich oligonucleotides inhibited the growth of xenograft tumors in mice,[33,35] an effect that can be explained by the antiangiogenic property of G-rich oligonucleotides unveiled here.

In the case of dextran sulfate and Fucoidan, molecular weight was found to be critical to their activity as NRP1 inhibitors in endothelial cells. Dextran sulfate (500 kDa; DS500) and Fucoidan effectively reduced NRP1 levels, but 8-kDa dextran sulfate and low molecular weight Fucoidan did not.[18] In the current study, we found that relatively short oligomers of G, including G18 and G6 are as active as poly G at reducing NRP1 levels in endothelial cells. It is possible that short G oligomers, like G6 or G18, assemble into 4-stranded helices stabilized by inter- and intramolecular hydrogen-bonded G-quartets. This 4 helices conformation of G is known to be a structural determinant for poly or oligo nucleotide binding to scavenger receptors, and it was suggested that the spatial distribution of negatively charged phosphates in nucleotide quadruplexes can provide a negatively charged surface for interaction with the positively charged surface of scavenger receptors.[24] The positively charged residues within the b1/b2 domain of NRP1 may similarly provide a surface for poly G or oligo G interaction, resulting in the oligo G-mediated linkage of scavenger receptor and NRP1. It was reported that a G10 oligomer can form aggregates, which contain between 20 and 30 molecules of monomeric G10.[38] Although we have not investigated the structure of G18 and G6 used in this study, it is possible that the bridging of NRP1 and scavenger receptor requires the formation of G18 multimers with higher molecular weight than single G18 or G6 molecules.

In view of the fact that NRP1 and NRP2 have the same domain structure,[39] it is interesting that oligo G did not reduce NRP2 levels on endothelial cells. This suggests that the charged side chains within the b1/b2 domain of NRP1, which differ from those in NRP2, play a critical role in the binding of oligo G. This selectivity of oligo G for NRP1 versus NRP2 is consistent with our results showing that oligo G does not indiscriminately reduce levels of endothelial cell-surface molecule. We cannot exclude, however, the possibility that, oligo G may target other molecules that we have not tested for. In particular, it is likely that oligo G can bind other scavenger receptors on endothelial cells besides SREC-I, as such cells express various scavenger receptors.[20,40] Although we have found that SREC-I is frequently internalized in conjunction with NRP1 under the conditions we have used, other scavenger receptors expressed by endothelial cells may also be concomitantly internalized or may substitute for SREC-I under different conditions.

Future development of oligo G as an internalization inducer may require methods to increase its specificity for the targeted molecule. One such method could involve the conjugation of oligo G with target-specific capture molecules, such as an antibody or small molecule that can specifically bind to cell-surface receptors. In this application, the capture-oligo G heterobifunctional molecules could be designed to induce specific internalization of selected target receptors to specifically block ligand-induced receptor signaling.

Authorship

Contribution: M.N., G.T., and X.L. designed research, performed experiments, analyzed data, and wrote the manuscript; and M.S., X.H., and T.T. performed some of the experiments and provided intellectual input to the experiments and manuscript.

Conflict-of-interest disclosure: The authors declare no competing financial interests.

Correspondence: Giovanna Tosato, Laboratory of Cellular Oncology, Center for Cancer Research, National Cancer Institute, National Institutes of Health, Bldg 37, Rm 4124, Bethesda, MD 20892-1907; e-mail: tosatog@mail.nih.gov.

References

1. Ferrara N, Gerber HP, LeCouter J. The biology of VEGF and its receptors. *Nat Med.* 2003;9(6):669-676.

2. Gumbiner BM. Cell adhesion: the molecular basis of tissue architecture and morphogenesis. *Cell.* 1996;84(3):345-357.

3. Rehman AO, Wang CY. Notch signaling in the regulation of tumor angiogenesis. *Trends Cell Biol.* 2006;16(6):293-300.

4. Ferguson SS. Evolving concepts in G protein-coupled receptor endocytosis: the role in receptor desensitization and signaling. *Pharmacol Rev.* 2001;53(1):1-24.

5. Levine SJ. Molecular mechanisms of soluble cytokine receptor generation. *J Biol Chem.* 2008; 283(21):14177-14181.

6. Zohlnhofer D, Graeve L, Rose-John S, Schooltink H, Dittrich E, Heinrich PC. The hepatic interleukin-6 receptor. Down-regulation of the interleukin-6 binding subunit (gp80) by its ligand. *FEBS Lett.* 1992;306(2-3):219-222.

7. He Z, Tessier-Lavigne M. Neuropilin is a receptor for the axonal chemorepellent Semaphorin III. *Cell.* 1997;90(4):739-751.

8. Kolodkin AL, Levengood DV, Rowe EG, Tai YT, Giger RJ, Ginty DD. Neuropilin is a semaphorin III receptor. *Cell.* 1997;90(4):753-762.

9. Soker S, Takashima S, Miao HQ, Neufeld G, Klagsbrun M. Neuropilin-1 is expressed by endothelial and tumor cells as an isoform-specific receptor for vascular endothelial growth factor. *Cell.* 1998;92(6):735-745.

10. Kawasaki T, Kitsukawa T, Bekku Y, et al. A requirement for neuropilin-1 in embryonic vessel formation. *Development.* 1999;126(21):4895-4902.

11. Pan Q, Chanthery Y, Liang WC, et al. Blocking neuropilin-1 function has an additive effect with anti-VEGF to inhibit tumor growth. *Cancer Cell.* 2007;11(1):53-67.

12. Takagi S, Hirata T, Agata K, Mochii M, Eguchi G, Fujisawa H. The A5 antigen, a candidate for the neuronal recognition molecule, has homologies to complement components and coagulation factors. *Neuron.* 1991;7(2):295-307.

13. Gu C, Limberg BJ, Whitaker GB, et al. Characterization of neuropilin-1 structural features that confer binding to semaphorin 3A and vascular endothelial growth factor 165. *J Biol Chem.* 2002; 277(20):18069-18076.

14. Mamluk R, Gechtman Z, Kutcher ME, Gasiunas N, Gallagher J, Klagsbrun M. Neuropilin-1 binds vascular endothelial growth factor 165, placenta growth factor-2, and heparin via its b1b2 domain. *J Biol Chem.* 2002;277(27):24818-24825.

15. Narazaki M, Tosato G. Ligand-induced internalization selects use of common receptor neuropilin-1 by VEGF165 and semaphorin3A. *Blood.* 2006;107(10):3892-3901.

16. Karpanen T, Heckman CA, Keskitalo S, et al. Functional interaction of VEGF-C and VEGF-D with neuropilin receptors. *FASEB J.* 2006;20(9): 1462-1472.

17. Vander Kooi CW, Jusino MA, Perman B, Neau DB, Bellamy HD, Leahy DJ. Structural basis for ligand and heparin binding to neuropilin B domains. *Proc Natl Acad Sci U S A.* 2007; 104(15):6152-6157.

18. Narazaki M, Segarra M, Tosato G. Sulfated polysaccharides identified as inducers of neuropilin-1 internalization and functional inhibition of VEGF165 and semaphorin3A. *Blood.* 2008; 111(8):4126-4136.

19. Adachi H, Tsujimoto M, Arai H, Inoue K. Expression cloning of a novel scavenger receptor from human endothelial cells. *J Biol Chem.* 1997; 272(50):31217-31220.

20. Adachi H, Tsujimoto M. Endothelial scavenger receptors. *Prog Lipid Res.* 2006;45(5):379-404.

21. Dhaliwal BS, Steinbrecher UP. Scavenger receptors and oxidized low density lipoproteins. *Clin Chim Acta.* 1999;286(1-2):191-205.

22. Platt N, Gordon S. Is the class A macrophage scavenger receptor (SR-A) multifunctional? The mouse's tale. *J Clin Invest.* 2001;108(5):649-654.

23. Li Y, Zhang F, Nagai N, et al. VEGF-B inhibits apoptosis via VEGFR-1-mediated suppression of the expression of BH3-only protein genes in mice and rats. *J Clin Invest.* 2008;118(3):913-923.

24. Pearson AM, Rich A, Krieger M. Polynucleotide binding to macrophage scavenger receptors depends on the formation of base-quartet-stabilized four-stranded helices. *J Biol Chem.* 1993;268(5): 3546-3554.

25. Gavard J, Hou X, Qu Y, et al. A role for a CXCR2/ phosphatidylinositol 3-kinase gamma signaling axis in acute and chronic vascular permeability. *Mol Cell Biol.* 2009;29(9):2469-2480.

26. Scheppke L, Aguilar E, Gariano RF, et al. Retinal vascular permeability suppression by topical application of a novel VEGFR2/Src kinase inhibitor in mice and rabbits. *J Clin Invest.* 2008;118(6): 2337-2346.

27. Nishimoto N, Kishimoto T. Interleukin 6: from bench to bedside. *Nat Clin Pract Rheumatol.* 2006;2(11):619-626.

28. Pastore C, Picchio GR, Galimi F, et al. Two mechanisms for human immunodeficiency virus type 1 inhibition by N-terminal modifications of RANTES. *Antimicrob Agents Chemother.* 2003; 47(2):509-517.

29. Murga M, Fernandez-Capetillo O, Tosato G. Neuropilin-1 regulates attachment in human endothelial cells independently of vascular endothelial growth factor receptor-2. *Blood.* 2005; 105(5):1992-1999.

30. Shimizu M, Murakami Y, Suto F, Fujisawa H. Determination of cell adhesion sites of neuropilin-1. *J Cell Biol.* 2000;148(6):1283-1293.

31. Guvakova MA, Yakubov LA, Vlodavsky I, Tonkinson JL, Stein CA. Phosphorothioate oligodeoxynucleotides bind to basic fibroblast growth factor, inhibit its binding to cell surface receptors, and remove it from low affinity binding sites on extracellular matrix. *J Biol Chem.* 1995; 270(6):2620-2627.

32. Pugh CW, Ratcliffe PJ. Regulation of angiogenesis by hypoxia: role of the HIF system. *Nat Med.* 2003;9(6):677-684.

33. Jing N, Li Y, Xiong W, Sha W, Jing L, Tweardy DJ. G-quartet oligonucleotides: a new class of signal transducer and activator of transcription 3 inhibitors that suppresses growth of prostate and breast tumors through induction of apoptosis. *Cancer Res.* 2004;64(18):6603-6609.

34. Xu Q, Briggs J, Park S, et al. Targeting Stat3 blocks both HIF-1 and VEGF expression induced by multiple oncogenic growth signaling pathways. *Oncogene.* 2005;24(36):5552-5560.

35. Guan Y, Reddy KR, Zhu Q, et al. G-rich oligonucleotides inhibit HIF-1alpha and HIF-2alpha and block tumor growth. *Mol Ther.* 2010;18(1):188-197.

36. Ferrara N. Role of myeloid cells in vascular endothelial growth factor-independent tumor angiogenesis. *Curr Opin Hematol.* 2010;17(3):219-224.

37. Kubota Y, Takubo K, Shimizu T, et al. M-CSF inhibition selectively targets pathological angiogenesis and lymphangiogenesis. *J Exp Med.* 2009; 206(5):1089-1102.

38. Chung IK, Muller MT. Aggregates of oligo(dG) bind and inhibit topoisomerase II activity and induce formation of large networks. *J Biol Chem.* 1991;266(15):9508-9514.

39. Geretti E, Shimizu A, Klagsbrun M. Neuropilin structure governs VEGF and semaphorin binding and regulates angiogenesis. *Angiogenesis.* 2008; 11(1):31-39.

40. Tamura Y, Adachi H, Osuga J, et al. FEEL-1 and FEEL-2 are endocytic receptors for advanced glycation end products. *J Biol Chem.* 2003; 278(15):12613-12617.